Submitted version of of: W. P. du Plessis, “Limiting Apparent Target Position in Skin-Return Influenced Cross-Eye Jamming,” *IEEE Transactions on Aerospace and Electronic Systems*, vol. 49, no. 3, pp. 2097-2101, July 2013. Published version is available online at: http://ieeexplore.ieee.org/arnumber=6558044

ABBREVIATIONS

JSR jammer-to-signal ratio

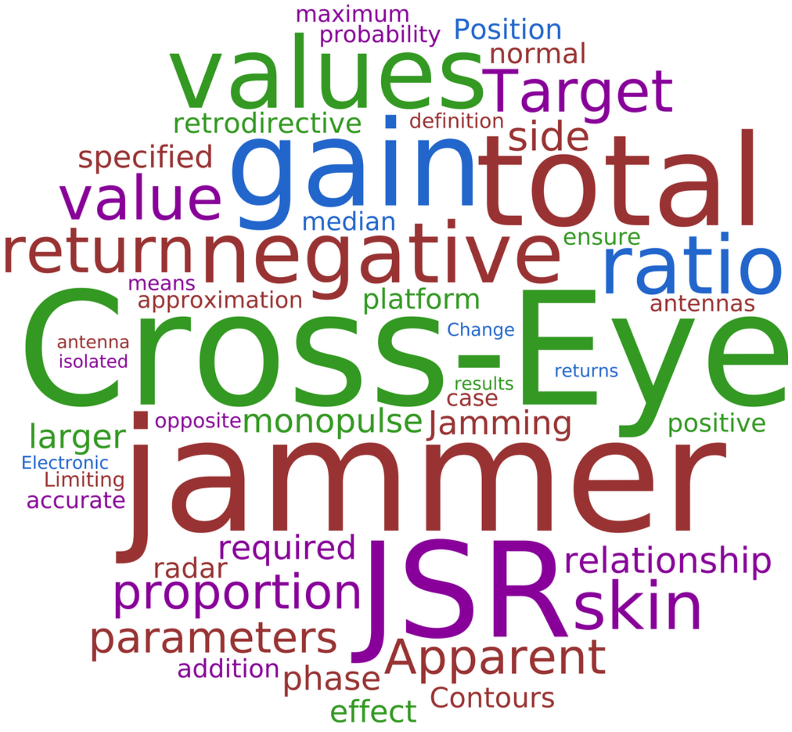

Limiting Apparent Target Position in Skin-Return Influenced Cross-Eye Jamming

W. P. du Plessis, *Senior Member, IEEE*

Abstract

It is desirable to limit the apparent target to one side of a retrodirective cross-eye jammer despite the variation caused by platform skin return. The relationship between the jammer parameters and the jammer-to-signal ratio (JSR) to ensure that this occurs is investigated. When this relationship is not satisfied, the proportion of the apparent targets generated on the opposite side of the jammer is determined.

Index Terms

Cross-eye jamming, electronic warfare (EW), electronic countermeasures (ECM), radar countermeasures, and monopulse radar.

I. Introduction

Cross-eye jamming is a radar countermeasure that seeks to deceive a threat radar as to the true position of its target by attempting to recreate the worst-case glint angular error [1]–[6]. The origin of the cross-eye jamming concept has meant that glint analyses have traditionally been reused for cross-eye jamming. However, glint analyses ignore the retrodirective implementation of cross-eye jamming, which appears to be the only way to overcome the extreme tolerance requirements associated with other implementations [2], [4], [6]. This ommission can lead to significant inaccuracies including the widespread belief that a retrodirective cross-eye jammer cannot break a tracking radar's lock (e.g. [1]–[4]), while a more complete analysis has shown that this is indeed possible [6]–[8].

The effect of platform skin return on a retrodirective cross-eye jammer has been analysed [9], and the widely quoted requirement of a JSR of 20 dB for effective cross-eye jamming (e.g. [4], [5]) was shown to be reasonable, though slightly conservative. However, the fact that the phase of a platform's skin return is inherently unknown means that the position of the apparent target is a distribution rather than a single value [9].

The complexity of the distribution of the apparent-target position presented in [9] meant that only the median of the position distribution could be considered in detail. While useful, these results are limited because tracking filters will not necessarily track the median position of a target. This paper attempts to address this limitation by considering the extreme edge of the position distribution in more detail.

Manuscript received February 3, 2012; revised May 23, 2012. This work was supported by the Armaments Corporation of South Africa (Armscor) under contract KT521896.

W. P. du Plessis is with the University of Pretoria, Lynnwood Road, Pretoria, Gauteng, 0002, South Africa (e-mail: wduplessis@ieee.org).

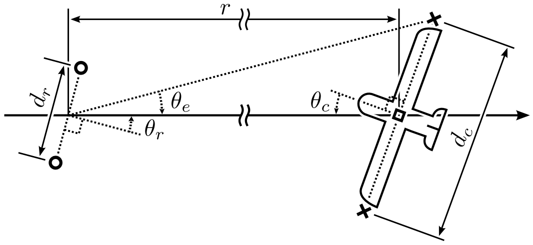

Fig. 1. The geometry of the cross-eye jamming scenario considered in [9]. The antenna-element phase centres of the phase-comparison monopulse radar and the jammer are denoted by circles and crosses respectively, and the point target used to model the platform skin return is denoted by a square.

The relationship between the JSR and the jammer parameters which will ensure that the apparent target is limited to one side of the jammer is presented. This condition is important because it marks the boundary beyond which it is no longer possible for the apparent target to be in the same direction as the true skin return. The jammer parameter tolerances and/or JSR required to achieve this condition are likely to prove prohibitive in practice. The proportion of the returns generated on the opposite side of the jammer to the desired apparent target for a specified relationship between the JSR and the jammer parameters is also presented. This proportion allows the performance degradation as a result of practical implementation constraints to be evaluated in a quantitative way.

II. Analysis

The geometry of a typical cross-eye engagement shown in Fig. 1 is used in the derivations below.

The monopulse ratio of a retrodirective cross-eye jammer in the presence of platform skin return positioned halfway between the jammer antennas is given by [9]

$$M_t \approx \tan(k) + G_{Ct}\frac{\sin(2k_c)}{\cos(2k)+1} \tag{1}$$

$$= \frac{\sin(2k) + G_{Ct}\sin(2k_c)}{\cos(2k)+1} \tag{2}$$

with

$$k \approx \beta\frac{d_r}{2}\sin(\theta_r) \tag{3}$$

$$k_c \approx \beta\frac{d_r}{2}\cos(\theta_r)\,\theta_e \tag{4}$$

where β is the free-space propagation constant and where the approximations are extremely accurate for typical cross-eye engagements where $d_c \ll r$. The total cross-eye gain is given by

$$G_{Ct} = \Re\left\{\frac{1-ae^{j\phi}}{1+ae^{j\phi}+a_s e^{j\phi_s}}\right\} \tag{5}$$

where a and ϕ are the amplitude and phase matching of the two signals transmitted by the jammer, and a_s and ϕ_s are the magnitude and phase of the skin return relative to the stronger of the two jammer returns.

The approximation in (1) is accurate when [9]

- the approximate form of k in (3) is accurate,

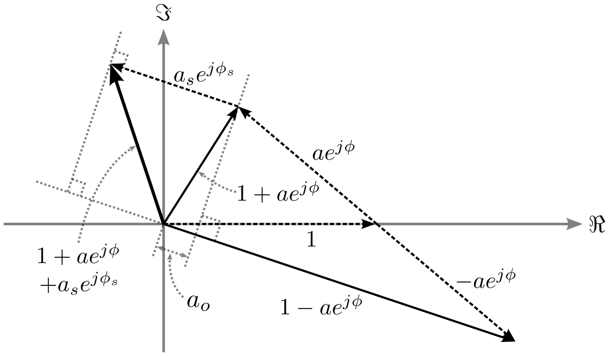

Fig. 2. Vector diagram for the numerator and denominator of the total cross-eye gain in (5).

- the characteristics of the radar antenna in the sum-channel main beam are primarily determined by the separation of the antenna elements,
- the jammer antennas have beamwidths which are much broader than the angular separation of the antenna elements (θ_e), and
- the separation of the jammer antennas is small enough to assume $\cos(2k_c) \approx 1$.

The JSR of the cross-eye jammer is given by [9]

$$\text{JSR} = a_s^{-2} \tag{6}$$

and can be related to the system parameters using equations given in [3], [9].

The phase of the platform skin return is inherently unknown and variable [9], so G_{Ct} in (5) is a distribution. The median value of G_{Ct} is [9]

$$G_{Ctm} = \frac{1 - a^2}{1 + a^2 + 2a\cos(\phi) + a_s^2} \tag{7}$$

when all values of ϕ_s are equally likely.

Remarkably, the forms of the monopulse ratio and cross-eye gain for the isolated case without platform skin return [6]–[8] are identical to (2) and (7), but for two minor differences. Firstly, $a_s = 0$ in the absence of skin return, reducing G_{Ct} to the same form as in the isolated case. The second difference is that the 1 in the denominator of (2) is $\cos(2k_c)$ in the isolated case, but the final assumption inherent in (2) means that this difference is unimportant. The main effect of the addition of skin return in the median case is thus only to modify the cross-eye gain to the form in [9].

The sign of M_t when the threat radar is tracking the centre of the jammer ($\theta_r = 0$) and the side of jammer where the monopulse ratio becomes zero depend on the sign of the second term on the right-hand side of (1). The sign of this term depends on the sign of G_{Ct} because the factor $\sin(2k_c) / [\cos(2k) + 1]$ is always positive in the sum-channel main beam [10]. The isolated cross-eye gain is positive when $a < 1$ (as assumed in [6]–[10]), so the G_{Ct} must be negative to produce an apparent target on the opposite side of the jammer to the desired apparent target.

A negative value of G_{Ct} can only be obtained when the phases of the complex numerator and denominator of (5) differ by more than 90°. As shown in Fig. 2, this condition requires the complex denominator of (5) to have a component in the opposite direction to the complex numerator of (5). The relevant component is maximised when ϕ_s is chosen to be in the opposite direction to $1 - ae^{j\phi}$ as shown in Fig. 2.

Fig. 2 shows that the value of G_{Ct} can thus only be negative when a_s is greater than the projection of $1 + ae^{j\phi}$ onto $1 - ae^{j\phi}$. This projection is denoted a_o and is given by

$$a_o = \left|1 + ae^{j\phi}\right| \cos\left(\phi_n - \phi_d\right) \tag{8}$$

$$= \frac{\left|1 + ae^{j\phi}\right| \left|1 - ae^{j\phi}\right| \cos\left(\phi_n - \phi_d\right)}{\left|1 - ae^{j\phi}\right|} \tag{9}$$

$$= \frac{\Re\left\{\left(1 + ae^{j\phi}\right)\left(1 - ae^{j\phi}\right)^*\right\}}{\left|1 - ae^{j\phi}\right|} \tag{10}$$

$$= \frac{1 - a^2}{\sqrt{1 + a^2 - 2a\cos\left(\phi\right)}} \tag{11}$$

where z^* denotes the complex conjugate of z, and ϕ_n and ϕ_d are the phases of the complex denominator and numerator of (5) respectively with $a_s = 0$. The value of G_{Ct} is thus limited to positive values when $a_s < a_o$, thereby limiting the apparent target position to one side of the jammer.

Substituting the value of a_o from (11) into (6) gives

$$\text{JSR}_o = \frac{1 + a^2 - 2a\cos\left(\phi\right)}{\left(1 - a^2\right)^2} \tag{12}$$

where JSR_o is the minimum JSR required to ensure that the apparent target is limited to one side of the jammer.

When the JSR is less than JSR_o, the apparent target will be generated on the opposite side of the jammer to the desired target when

$$a_s \cos\left(\phi_n - \phi_d\right) + a_o < 0\ . \tag{13}$$

The value of $\phi_n - \phi_s$ that makes this projection equal to a_o can be determined from

$$a_s \cos\left(\phi_n - \phi_d\right) = -a_o \tag{14}$$

$$\phi_o = \pi - \arccos\left(\frac{a_o}{a_s}\right) \tag{15}$$

where ϕ_o is the value of $\phi_n - \phi_d$ which gives a zero projection. G_{Ct} is thus negative when $|\phi_n - \phi_d| > |\phi_o|$. Given that $|\phi_n - \phi_d| \in [0, \pi]$, only the range $[\phi_o, \pi]$ of the complete $[0, \pi]$ range of $|\phi_n - \phi_d|$ gives negative G_{Ct} values. The probability that G_{Ct} is negative is thus given by

$$P\left(G_{Ct} < 0\right) = \frac{\pi - \phi_o}{\pi} \tag{16}$$

$$= \frac{1}{\pi} \arccos\left(\frac{a_o}{a_s}\right) \tag{17}$$

which can be rewritten as

$$\frac{1}{a_s} = \frac{\cos\left[\pi P\left(G_{Ct} < 0\right)\right]}{a_o} \tag{18}$$

$$\text{JSR}_{P(G_{Ct}<0)} = \text{JSR}_o \cos^2\left[\pi P\left(G_{Ct} < 0\right)\right] \tag{19}$$

where $\text{JSR}_{P(G_{Ct}<0)}$ denotes the JSR to ensure a specified $P\left(G_{Ct} < 0\right)$.

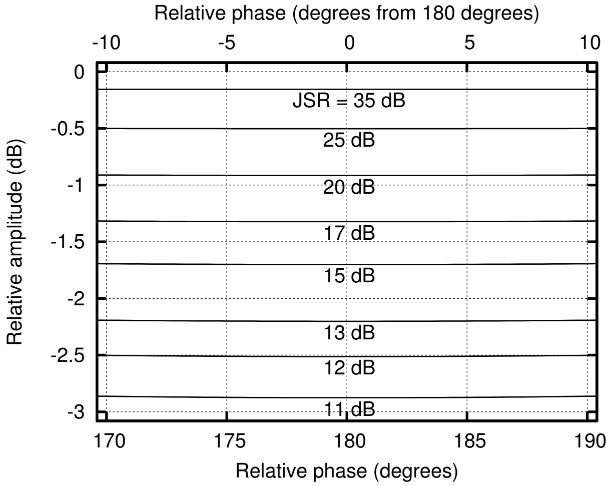

Fig. 3. Contours showing the relationship between the jammer parameters and the JSR to ensure that the total cross-eye gain is always positive.

III. Discussion

The first important result above is captured in (11) and (12), which allow the minimum JSR required to ensure that G_{Ct} is positive for a given set of jammer parameters to be computed. This figure of merit is illustrated in Fig. 3 by plotting contours of the maximum value of a required to ensure that G_{Ct} is strictly positive for the specified JSR values using (12).

The main conclusion from the contours in Fig. 3 is that higher JSR values allow larger values of a while maintaining a positive G_{Ct}. This follows directly from Fig. 2 where a smaller value of a_s (higher JSR) means that a smaller value of a_o is required, thereby allowing a larger value of a.

A further observation is that greater JSR increases are required to achieve a specified improvement in a for larger JSR values. This situation arises because the relationship between a and a_o is highly nonlinear as shown in (11). With reference to Fig. 2, modifying a_o (and thus the JSR) has a larger effect on the maximum allowable value of a when a_o is a larger proportion of a.

Lastly, the contours associated with each JSR value are approximately constant in Fig. 3 because $\cos(\phi) \approx -1$ to over the range of ϕ values considered. This means that (12) can be simplified to

$$\mathrm{JSR}_o \approx (1-a)^{-2} \tag{20}$$

to a high degree of accuracy for cross-eye jamming where $\phi \approx 180°$.

The second important result derived above is described by (19), which gives the relationship between the jammer system parameters and the proportion of apparent targets on the opposite side of the jammer to the desired apparent target (negative G_{Ct}). Increasing the proportion of the apparent targets on the opposite side of the jammer allows either a lower JSR for a given set of jammer parameters or the jammer parameters corresponding to a higher JSR_o to be used. In both cases, the factor $\cos^2[\pi P(G_{Ct} < 0)]$ determines the JSR change.

The first possibility mentioned above means that the JSR values associated with the contours in Fig. 3 are decreased by 0.44 dB, 1.84 dB, 4.62 dB and 10.20 dB when 10%, 20%, 30% and 40% of the G_{Ct} values

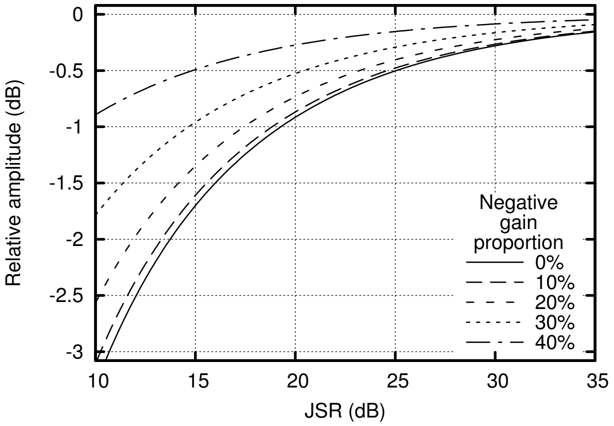

Fig. 4. The relationship between the jammer transmitter amplitudes and the JSR required to achieve a specified proportion of results with negative total cross-eye gain.

are negative respectively. From these values it is clear that the nonlinear nature of the cosine function in (19) means changes to $P\left(G_{Ct}<0\right)$ have a larger effect on the jammer parameters when $P\left(G_{Ct}<0\right)$ is larger.

The second possibility is explored in Fig. 4 where contours of the maximum a values associated with a number of JSR values are plotted when a specified proportion of G_{Ct} may be negative under the assumption that $\phi \approx$180°. In all cases, allowing some negative G_{Ct} values increases the maximum allowable value of a, as shown in (19).

The increase in the maximum allowable a value caused by accepting a higher proportion of negative G_{Ct} values in Fig. 4 decreases as the JSR increases. As before, this occurs because a_s is a larger proportion of a when the JSR is low, so any change to a_s has a greater effect on a at low JSR values.

Fig. 4 also supports the earlier observation that changing the proportion of G_{Ct} values which are allowed to be negative has a smaller effect on the jammer parameters when $P\left(G_{Ct}<0\right)$ is low. This is again due to the nonlinear nature of the cosine in (19).

Fig. 5 shows the curves in Fig. 4 as a function of both a and ϕ as well as the constant median total cross-eye gain (G_{Ctm}) contours from [9] for a 15-dB JSR.

The fact that the constant G_{Ctm} curves intersect the maximum a curves in Fig. 5 shows that it is possible to achieve a specified G_{Ctm} with or without allowing negative G_{Ct} values. For example, a $G_{Ctm}=5$ can be achieved with no negative G_{Ct} values near the bottom of the relevant constant-gain contour, while negative G_{Ct} values are possible near the top of the relevant constant-gain contour. This characteristic is explained by the fact that the cross-eye jammer has a larger sum-channel component when a is smaller, thereby reducing the effect of the platform's skin return and leading to a smaller G_{Ct} variation [9].

An important consequence of the curves in Fig. 5 is that finer tolerances may be required from a retrodirective cross-eye jammer system if a specified minimum G_{Ct} value is to be achieved while limiting the proportion of negative G_{Ct} values. For example, when $\phi=180°$, ensuring a minimum G_{Ctm} of 5 requires -1.99 dB $\leq a \leq$ -1.20 dB [9], while (19) and (20) show that limiting 0%, 10% and 20% of G_{Ct} values to be negative reduces the upper end of this range to -1.70 dB, -1.61 dB and -1.35 dB respectively. There is no change to the allowable upper value of a when at least 24.2% of G_{Ct} values may be negative because these contours do not

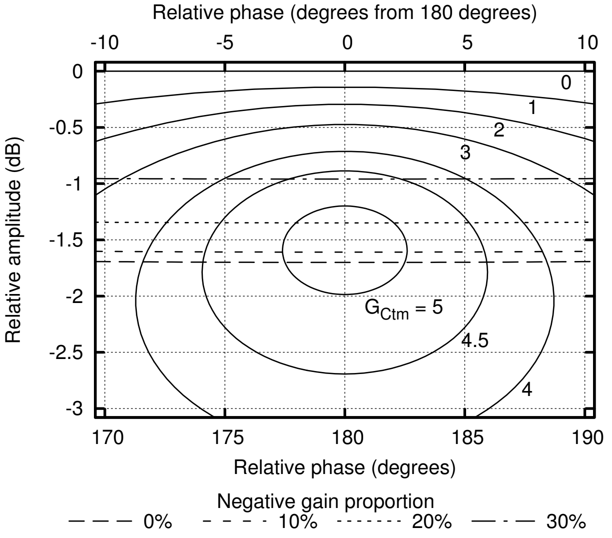

Fig. 5. Contours of constant median total cross-eye gain from [9] (solid lines) and the specified proportion of negative total cross-eye gain values for a 15-dB JSR.

intersect the $G_{Ctm} = 5$ contour.

IV. Conclusion

The relationship between the JSR and the jammer parameters required to ensure that the apparent target generated by the cross-eye jammer is limited to one side of the jammer was determined. This desirable situation occurs when the total cross-eye gain is limited to only positive values. The jammer parameters were shown to be insensitive to the jammer phase over the range of parameter values considered, and an accurate approximation to the relationship between the JSR and the jammer channel amplitude matching was derived.

The relationship between the JSR and the jammer parameters when a specified proportion of the total cross-eye gain values are negative was also derived. The effect of this change is simply to reduce the JSR required by a factor dependent only on the allowable negative total cross-eye gain proportion. This factor is highly nonlinear with the JSR reduction initially being small, but increasing rapidly.

It was also shown that limiting the total cross-eye gain to positive values can require significantly finer tolerances from a retrodirective cross-eye jammer system. These tolerances are eased as larger proportions of the total cross-eye gain values are allowed to be negative.

Acknowledgment

The author wishes to express his sincere thanks the anonymous reviewers, whose insightful comments and suggestions greatly enhanced this paper.

References

[1] S. A. Vakin and L. N. Shustov, “Principles of jamming and electronic reconnaissance – Volume I,” U.S. Air Force, Tech. Rep. FTD-MT-24-115-69, AD692642, 1969.

[2] L. B. Van Brunt, *Applied ECM*. EW Engineering, Inc., 1978, vol. 1.

[3] A. Golden, *Radar Electronic Warfare*. AIAA Inc., 1987.

[4] D. C. Schleher, *Electronic warfare in the information age*. Artech House, 1999.

[5] F. Neri, *Introduction to Electronic Defense Systems*, 2nd ed. SciTech Publishing, 2006.

[6] W. P. du Plessis, "A comprehensive investigation of retrodirective cross-eye jamming," Ph.D. dissertation, University of Pretoria, 2010.

[7] W. P. du Plessis, J. W. Odendaal, and J. Joubert, "Extended analysis of retrodirective cross-eye jamming," *IEEE Trans. Antennas Propag.*, vol. 57, no. 9, pp. 2803–2806, September 2009.

[8] W. P. du Plessis, J. W. Odendaal, and J. Joubert, "Experimental simulation of retrodirective cross-eye jamming," *IEEE Trans. Aerosp. Electron. Syst.*, vol. 47, no. 1, pp. 734–740, January 2011.

[9] W. P. du Plessis, "Platform skin return and retrodirective cross-eye jamming," *IEEE Trans. Aerosp. Electron. Syst.*, vol. 48, no. 1, pp. 490–501, January 2012.

[10] W. P. du Plessis, J. W. Odendaal, and J. Joubert, "Tolerance analysis of cross-eye jamming systems," *IEEE Trans. Aerosp. Electron. Syst.*, vol. 47, no. 1, pp. 740–745, January 2011.